



## Isotope correlations as a probe for freeze-out characterization: central $^{124}\text{Sn}+^{64}\text{Ni}$ , $^{112}\text{Sn}+^{58}\text{Ni}$ collisions

E. Geraci, M. Alderighi, A. Anzalone, L. Auditore, V. Baran, M. Bartolucci, I. Berceanu, J. Blicharska, A. Bonasera, B. Borderie, et al.

### ► To cite this version:

E. Geraci, M. Alderighi, A. Anzalone, L. Auditore, V. Baran, et al.. Isotope correlations as a probe for freeze-out characterization: central  $^{124}\text{Sn}+^{64}\text{Ni}$ ,  $^{112}\text{Sn}+^{58}\text{Ni}$  collisions. International Conference on Nucleus-Nucleus Collisions (NN2003) 8, Jun 2003, Moscow, Russia. pp.524-527. in2p3-00021661

**HAL Id: in2p3-00021661**

**<https://hal.in2p3.fr/in2p3-00021661>**

Submitted on 16 Apr 2004

**HAL** is a multi-disciplinary open access archive for the deposit and dissemination of scientific research documents, whether they are published or not. The documents may come from teaching and research institutions in France or abroad, or from public or private research centers.

L'archive ouverte pluridisciplinaire **HAL**, est destinée au dépôt et à la diffusion de documents scientifiques de niveau recherche, publiés ou non, émanant des établissements d'enseignement et de recherche français ou étrangers, des laboratoires publics ou privés.

# Isotope correlations as a probe for freeze-out characterization: central $^{124}\text{Sn}+^{64}\text{Ni}$ , $^{112}\text{Sn}+^{58}\text{Ni}$ collisions

E. Geraci<sup>a, b</sup>, M. Alderighi<sup>c</sup>, A. Anzalone<sup>b</sup>, L. Auditore<sup>d</sup>, V. Baran<sup>b,e</sup>, M. Bartolucci<sup>f</sup>, I. Berceanu<sup>e</sup>, J. Blicharska<sup>g</sup>, A. Bonasera<sup>b</sup>, B. Borderie<sup>h</sup>, R. Bougault<sup>i</sup>, M. Bruno<sup>a</sup>, J. Brzychczyk<sup>j</sup>, G. Cardella<sup>k</sup>, S. Cavallaro<sup>b</sup>, A. Chbihi<sup>l</sup>, J. Cibor<sup>m</sup>, M. Colonna<sup>b</sup>, M. D'Agostino<sup>a</sup>, E. De Filippo<sup>k</sup>, M. Di Toro<sup>b</sup>, F. Giustolisi<sup>b</sup>, A. Grzeszczuk<sup>g</sup>, P. Guazzoni<sup>f</sup>, D. Guinet<sup>n</sup>, M. Iacono-Manno<sup>b</sup>, S. Kowalski<sup>g</sup>, E. La Guidara<sup>b</sup>, G. Lanzalone<sup>b</sup>, G. Lanzanó<sup>k</sup>, N. Le Neindre<sup>h</sup>, S. Li<sup>o</sup>, S. Lo Nigro<sup>k</sup>, C. Maiolino<sup>b</sup>, Z. Majka<sup>j</sup>, G. Manfredi<sup>f</sup>, T. Paduszynski<sup>g</sup>, A. Pagano<sup>k</sup>, M. Papa<sup>k</sup>, M. Petrovici<sup>e</sup>, E. Piasecki<sup>p</sup>, S. Pirrone<sup>k</sup>, G. Politi<sup>k</sup>, A. Pop<sup>e</sup>, F. Porto<sup>b</sup>, M. F. Rivet<sup>h</sup>, E. Rosato<sup>q</sup>, S. Russo<sup>f</sup>, P. Russotto<sup>b</sup>, G. Sechi<sup>c</sup>, V. Simion<sup>e</sup>, M. L. Sperduto<sup>b</sup>, J. C. Steckmeyer<sup>i</sup>, A. Trifirò<sup>d</sup>, M. Trimarchi<sup>d</sup>, G. Vannini<sup>a</sup>, M. Vigilante<sup>q</sup>, J. P. Wieleczko<sup>l</sup>, J. Wilczynski<sup>r</sup>, H. Wu<sup>o</sup>, Z. Xiao<sup>o</sup>, L. Zetta<sup>f</sup>, W. Zipper<sup>g</sup>

<sup>a</sup> INFN and Dipartimento di Fisica, Università di Bologna, Italy

<sup>b</sup> INFN-LNS and Dipartimento di Fisica e Astronomia, Università di Catania, Italy

<sup>c</sup> INFN and Istituto di Fisica Cosmica, CNR, Milano, Italy

<sup>d</sup> INFN and Dipartimento di Fisica, Università di Messina, Italy

<sup>e</sup> Institute for Physics and Nuclear Engineering, Bucharest, Romania

<sup>f</sup> INFN and Dipartimento di Fisica, Università di Milano, Italy

<sup>g</sup> Institute of Physics, University of Silesia, Katowice, Poland

<sup>h</sup> Institut de Physique nucléaire, IN2P3-CNRS, Orsay, France

<sup>i</sup> LPC, ENSI Caen and Université de Caen, France

<sup>j</sup> M. Smoluchowski Institute of Physics, Jagellonian University, Cracow, Poland

<sup>k</sup> INFN and Dipartimento di Fisica e Astronomia, Università di Catania, Italy

<sup>l</sup> GANIL, CEA, IN2P3-CNRS, Caen, France

<sup>m</sup> H. Niewodniczanski Institute of Nuclear Physics, Cracov, Poland

<sup>n</sup> Institut de Physique nucléaire, IN2P3-CNRS, Lyon, France

<sup>o</sup> Institute of Modern Physics Lanzhou, China

<sup>p</sup> Institute of Experimental Physics, University of Warsaw, Poland

<sup>q</sup> INFN and Dipartimento di Fisica, Università di Napoli, Italy

<sup>r</sup> Institute for Nuclear Studies, Otwock-Swierk, Poland

$^{124}\text{Sn}+^{64}\text{Ni}$  and  $^{112}\text{Sn}+^{58}\text{Ni}$  reactions at 35 AMeV incident energy were studied with the forward part of CHIMERA multi-detector. The most central collisions were selected by means of a multidimensional analysis. The characteristics of the source formed in the central collisions, as size, temperature and volume, were inspected. The measured isotopes of light fragments ( $3 \leq Z \leq 8$ ) were used to examine isotope yield ratios that provide information on the free neutron to proton densities.

## 1. INTRODUCTION

The isotopic composition of nuclear reaction products provides important information on the reaction dynamics and the possible occurrence of a liquid-gas phase transition [1]. Isotopically resolved light fragments have revealed systematic scalings [2] that supply information on neutron and proton densities at the breakup stage. The isoscaling has been observed in a variety of reactions under the assumptions of statistical emissions and equal temperature and volume of the two considered systems. Our study was devoted to select central collisions, inspect the characteristics of the source formed in the central events (size, temperature and volume), and examine the isotopic ratios. In particular, using fragments with a charge  $3 \leq Z \leq 8$  identified in mass, we studied the isoscaling and the isotopic ratios for mirror nuclei. We present data concerning  $^{124}\text{Sn}+^{64}\text{Ni}$  and  $^{112}\text{Sn}+^{58}\text{Ni}$  central collisions at 35 AMeV. The measurements have been performed using the 688 Si-CsI telescopes of the forward part ( $1^\circ \leq \theta_{lab} \leq 30^\circ$ ) of CHIMERA apparatus in the framework of Reverse Experiments [3].

## 2. EVENT SELECTION AND SOURCE CHARACTERIZATION

In order to have an impact parameter selector we resorted to the principal component analysis (PCA), which is a multivariate analysis technique [4] concerned with determination of the so-called principal variables, linear combinations of the primary physical variables. In our case, the first three principal components (P1, P2, P3) define principal planes where the data retain about 80% of the original information. The experimental events, projected on the P1-P2 plane, show three well distinct clouds. Two bumps correspond to events that can be associated to peripheral collisions. The third cloud mostly contains well detected multifragmentation events, characterized by high IMF multiplicity. A variable summarizing both the information provided by P1 and P3 allows for a more careful selection in order to separate central and semi-peripheral collisions and to select events with an isotropic distribution of  $\cos(\Theta_{flow})$ .

To get information on the characteristics of the source, formed in central collisions, we performed a comparison between data and statistical model (SMM [5]) predictions. The statistical model reproduces quite well the experimental observables (Fig. 1) if, for n-poor (rich) reaction, a source is considered having mass  $A = 145(160)$ , charge  $Z = 66$ , excitation energy  $5\text{ AMeV}$  and a freeze-out volume of  $3V_0$ . These source characteristics are in good agreement with the predictions of the dynamical model BNV [6], which predicts for the n-poor (rich) reaction that an equilibrated excited system with  $A = 150(164)$ ,  $Z = 67(68)$  and  $E^*/A = 4.7(5.1)$  MeV is formed at a time 120-140 fm/c after the initial stage of the collision.

Information about the space-time evolution of the reaction zone has been obtained via intensity interferometry. The two-fragments velocity correlation function for IMFs ( $Z \geq 3$ ) reveals that the sources formed in  $^{124}\text{Sn}+^{64}\text{Ni}$  and  $^{112}\text{Sn}+^{58}\text{Ni}$  central collisions decay by emitting fragments and isotopes showing almost identical space-time patterns [7].

The temperatures of the two sources were extracted by looking at the double isotope ratios thermometers [8]. The temperature is given by  $T = \frac{B}{\ln(sR)}$  where  $s$  is related to the ground state spins,  $R$  is the ratio of the production yields of four isotopes and  $B$  is related to the isotope binding energies. The measured yields of isotopes from Lithium

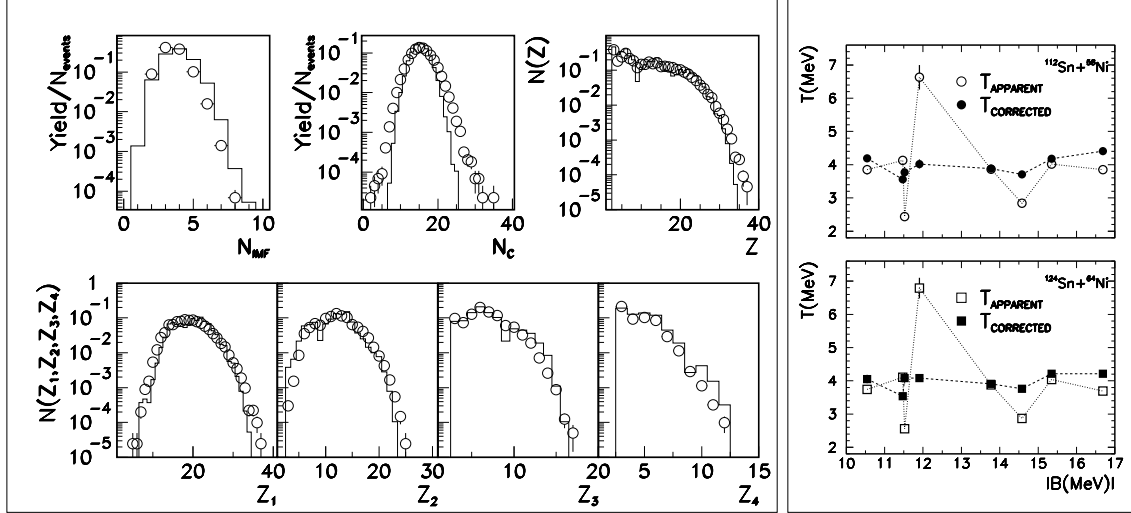


Figure 1. Left box: IMF multiplicity, total charged multiplicity, charge distribution and charge partition in each event ( $Z_1 \geq Z_2 \geq Z_3 \geq Z_4$ ). Circles represent data, lines SMM filtered predictions for central  $^{112}\text{Sn}+^{58}\text{Ni}$  collisions. Right box: The apparent and corrected temperatures as a function of the difference in binding energies for the  $^{112}\text{Sn}+^{58}\text{Ni}$  (top) and  $^{124}\text{Sn}+^{64}\text{Ni}$  (bottom) systems.

to Oxygen were used to construct the so-called apparent temperatures; their values and the values after secondary decay correction [9] are presented as a function of the binding energy term B in the right box of Fig. 1. The deduced values of the temperatures are in the range typical for reaction processes near the onset of multi-fragment emissions [9,10]. The weighted average corrected temperatures result  $3.96 \pm 0.04$  and  $3.94 \pm 0.03\text{MeV}$  for  $^{112}\text{Sn}+^{58}\text{Ni}$  and  $^{124}\text{Sn}+^{64}\text{Ni}$  reactions respectively.

### 3. ISOTOPES ANALYSIS

Having verified that the sources of the two analysed systems present the same size, temperature, volume and emission patterns, we moved on to study the isotopic ratios. In the Grand-Canonical approximation the yield ratio  $R_{21}$  of a fragment of N neutrons and Z protons, emitted in two reactions differing only in isospin, is related to the relative free neutron density and to the relative free proton density by the relation (neglecting the particle unstable feeding corrections [11]):

$$R_{21}(N, Z) = \frac{Y_{124\text{Sn}+64\text{Ni}}(N, Z)}{Y_{112\text{Sn}+58\text{Ni}}(N, Z)} = C \left( \frac{\rho_{n,2}}{\rho_{n,1}} \right)^N \left( \frac{\rho_{p,2}}{\rho_{p,1}} \right)^Z = C \hat{\rho}_n^N \hat{\rho}_p^Z.$$

C is an overall normalization factor and  $\hat{\rho}_n$ ,  $\hat{\rho}_p$  are the relative free neutron and proton densities, related to the isoscaling parameters  $\alpha$  and  $\beta$  [2]. In Fig. 2 the measured isotopic ratios are plotted as a function of neutron number (left upper panel) and proton number (left lower panel) of fragments. On the right panel of Fig. 2 the mirror isobar ratios are shown. If the sequential decay and the Coulomb effects are small, the dependence of isobaric mirror yield ratios on the binding energy difference should be exponential, i.e. of the form  $(\rho_n/\rho_p)_i \exp(\Delta B/T_i)$  where  $T_i$  is the temperature of the emitting source for the reaction  $i$  and  $(\rho_n)_i$  and  $(\rho_p)_i$  are the free neutron and proton densities for the same reaction. A constrained fit on the 27 experimental ratios of Fig. 2 has been performed. The average corrected isotope temperature is assumed as the temperature of the emitting systems. The relative neutron and proton densities  $\hat{\rho}_n$ ,  $\hat{\rho}_p$ , C and the free neutron to

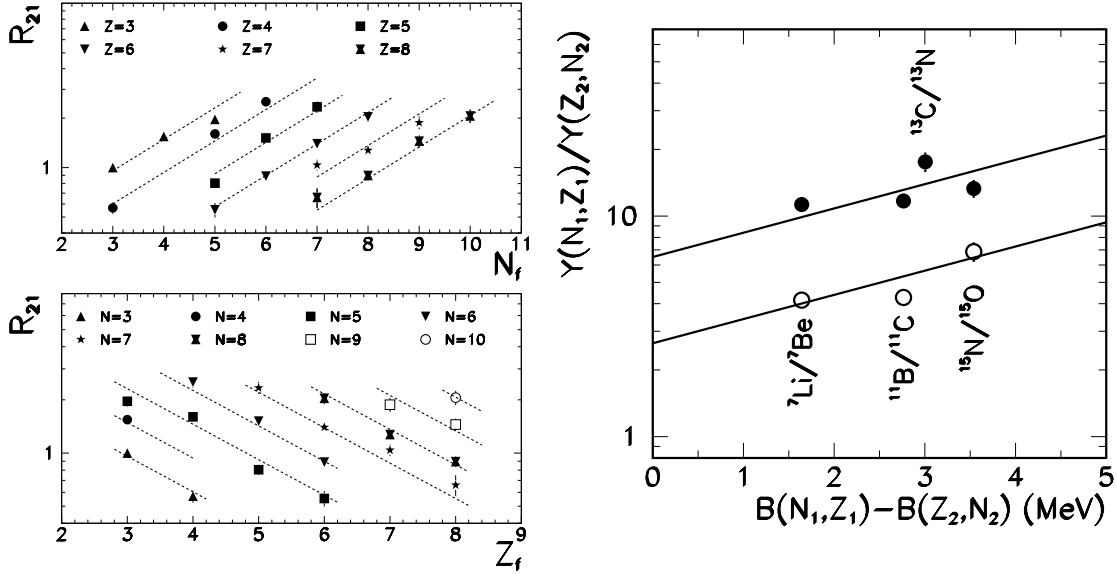


Figure 2. Left panels: Isotopic ratio  $R_{21}$  versus the neutron number  $N_f$  (top) and the proton number  $Z_f$  (bottom) of detected fragments. Right panel: Isobar ratios as a function of  $\Delta B$  for mirror nuclei in  $^{112}\text{Sn} + ^{58}\text{Ni}$  (open circles) and  $^{124}\text{Sn} + ^{64}\text{Ni}$  (solid points) reactions. Lines represent the result of the constrained fit.

proton density  $(\rho_n/\rho_p)_{124}$  (for the reaction  $^{124}\text{Sn} + ^{64}\text{Ni}$ ) were used as free parameters of the fit. The  $(\rho_n/\rho_p)$  for the reaction  $^{112}\text{Sn} + ^{58}\text{Ni}$  has been derived as  $(\rho_n/\rho_p)_{112} = (\rho_n/\rho_p)_{124} \cdot \hat{\rho}_p/\hat{\rho}_n$ . A very good agreement with an exponential behaviour has been obtained giving values  $\hat{\rho}_n = 1.55 \pm 0.02$ ,  $\hat{\rho}_p = 0.63 \pm 0.01$  (corresponding to isoscaling parameters  $\alpha = 0.44 \pm 0.01$  and  $\beta = -0.46 \pm 0.02$ ),  $(\rho_n/\rho_p)_{124} = 6.5 \pm 0.2$  and  $(\rho_n/\rho_p)_{112} = 2.6 \pm 0.1$ .

It can be observed that the extracted values of  $\hat{\rho}_n$  and  $(\rho_n/\rho_p)$  result definitely higher than the values calculated (1.08, 1.41 and 1.18) assuming neutrons and protons homogeneously distributed in a volume proportional to the nucleons number, supporting the idea of the isospin distillation mechanism. Even if this can be a signal expected for a liquid-gas phase transition further analyses are required to evaluate secondary decay effects.

## REFERENCES

1. *Isospin Physics in Heavy-Ion Collisions at Intermediate Energies*, edited by Bao-An Li and W.Udo Schröder, ISBN 1-56072-888-4, Nova Science Publ. Inc., New York (2001).
2. H. S. Xu *et al.*, Phys. Rev. Lett. **85** (2000) 716; M.B. Tsang *et al.*, Phys. Rev. Lett. **86** (2001) 5023; A.S. Botvina *et al.*, Phys. Rev. **C65** (2002) 044610.
3. A. Pagano *et al.*, Nucl. Phys. A681(2001) 331; A. Pagano *et al.*, contribution on this volume and references therein.
4. P. Desesquelles, Ann. Phys. Fr. 20 (1995) 1
5. J. Bondorf *et al.*, Phys. Rep. **257** (1995) 133.
6. M. Colonna, N. Colonna, A. Bonasera and M. Di Toro Nucl.Phys. **541** (1992) 295.
7. E. Geraci *et al.*, submitted to Nucl. Phys.
8. S. Albergo, S. Costa, E. Costanzo, and A. Rubbino, Il Nuovo Cimento 89 A (1985) 1.
9. M.B. Tsang, W.G. Lynch, H. Xi, and W.A. Friedman, Phys. Rev. Lett. **78** (1997) 3836.
10. J. Pochodzalla *et al.*, Phys. Rev. Lett. **75** (1995) 1040; J. B. Natowitz *et al.*, Phys. Rev. **C 65** (2002) 034618.
11. M. B. Tsang *et al.*, Phys. Rev. **C64** (2001) 054615.